Thermochimica Acta 474 (2008) 72–77

Contents lists available at ScienceDirect

Thermochimica Acta

journal homepage: www.elsevier.com/locate/tca

Non-isothermal degradation kinetics of MMA-St copolymer and EPS lost foams

Hamid Reza Azimi[a], Mostafa Rezaei[a,*], Farhang Abbasi[a], Ali Charchi[a], Yahya Bahluli[b]

[a] Institute of Polymeric Materials, Chemical Engineering Department, Sahand University of Technology, P.O. Box 51335-1996, Tabriz, Iran
[b] Metallurgical Research Center, Iran Tractor Foundry Company, Tabriz, Iran, P.O. Box 51845-338, Tabriz, Iran

ARTICLE INFO

Article history:
Received 27 February 2008
Received in revised form 20 May 2008
Accepted 25 May 2008
Available online 7 July 2008

Keywords:
Lost foam
MMA-St copolymer
EPS
Degradation kinetics

ABSTRACT

Methylmethacrylate-styrene (MMA-St) random copolymer was synthesized by suspension copolymerization. The thermal degradation of MMA-St copolymer and EPS lost foams was studied by non-isothermal thermal gravimetric analysis under nitrogen purge. Thermal decomposition behavior of MMA-St copolymer lost foam was examined and compared with EPS. It was found that EPS foam starts to decompose at higher temperatures than MMA-St copolymer foam in all heating rates. The apparent activation energy was calculated by the Flynn-Wall-Ozawa method. It has been concluded that the model fitting methods unable to reveal the complexity of the pyrolysis process and the model-free methods can be suggested as a reliable way of determining the kinetic parameters.

1. Introduction

The expandable pattern casting (EPC) or lost foam casting (LFC) is an economic and most widely used method to produce complex metal parts, in which the liquid metal displaced of refractory coated expandable foam patterns by means of thermal degradation. The LFC process is widely employed by the automotive industry for making engine components. Aluminum and iron casting are the most common; however, magnesium casting could be a potential replacement in high temperature applications because of its improved strength-to-weight ratio [1].

In this method the cast is made of expanded polystyrene (EPS) or styrene-methyl metacrylate (St-MMA) copolymer foam. Lost foam patterns are attached to a gating system and then a thin layer of refractory coating material is applied to the entire assembly. After the coating has been completely dried, the foam pattern is entirely imbedded in unbounded sand in the vented container. During the sand pouring cycle, vibration is applied to the flask to compact the sand [2].

This technology has different advantages compared to conventional casting methods in which the cast is made of EPS in aluminum casting or expanded methylmetacrylate-styrene (MMA-St) copolymer in iron casting [2]. Lustrous carbon defects are reduced in iron casting by using MMA-St copolymer foam compared to EPS. Thermal decomposition of polystyrene (PS), EPS and polymethyl methacrylate (PMMA) has been considered in some researches. In the virgin PS and EPS, the chain scission (depolymerization) is the main thermal degradation mechanism which produces styrene monomer, dimer and trimer, through an intrachain reaction [1,3]. The detectable product in PMMA thermal degradation, is monomer that strongly indicates a depropagation (unzipping) mechanism [4,5]. Furthermore the thermal degradation of PMMA has been studied under nitrogen and oxygen atmospheres in which the stabilizing effect of oxygen on the thermal degradation of PMMA has been reported [6]. The mechanism of thermal decomposition of MMA-St copolymer foam has not been considered so much before. In this work, the thermal degradation kinetics of MMA-St copolymer and EPS lost foams are investigated and compared.

Thermal gravimetric (TG) method has been extensively used for such studies. Experiments are usually performed under non-isothermal conditions. Several techniques are commonly used in the study of pyrolysis kinetics based on TG analysis. Isoconversional methods are reliable techniques which determine the activation energy at fixed conversions [7]. Some different kinetics models have been used for estimating the kinetics parameters of different polymers and copolymers [8–14]. Reaction mechanism fitting method which can provide some information on the reaction mechanism of pyrolysis [15,16], is used through the determination of the apparent activation energy. In this study, the activation energies of lost foam copolymer have been calculated using Flynn-Ozawa-Wall [17,18] method and compared with those for EPS. Furthermore the isokinetic relationship (IKR) was used to estimate a

* Corresponding author. Tel.: +98 412 3459086; fax: +98 412 3444355.
E-mail address: rezaei@sut.ac.ir (M. Rezaei).

0040-6031/$ – see front matter © 2008 Elsevier B.V. All rights reserved.
doi:10.1016/j.tca.2008.05.009

model-independent pre-exponential factor for each degree of conversion.

2. Theoretical background

The pyrolysis rate which is dependent on the time, temperature and mass change of the sample is defined as:

$$\frac{d\alpha}{dt} = k(T)f(\alpha) \quad (1)$$

where α is the degree of conversion and commonly defined as; $\alpha = (w_0 - w_t)/(w_0 - w_f)$ in which w_0, w_t and w_f are the initial, actual and final weight of the sample, respectively; t is the time, $f(\alpha)$ is the differential conversion function (kinetics model) and $k(T)$ is the temperature dependent rate constant, which can be expressed by the Arrhenius equation:

$$k = Ae^{-E/RT} \quad (2)$$

where E is the activation energy (J/mol), A is the pre-exponential factor (s^{-1}) and R is the gas constant (8.314 J/mol K). The kinetics analysis of non-isothermal data is generally performed by the following equation [19]:

$$\frac{d\alpha}{dt} = \beta\frac{d\alpha}{dT} = Af(\alpha)\exp\left(\frac{-E}{RT}\right) \quad (3)$$

where, β ($\beta = dT/dt$) is the constant heating rate.

Rearrangement of Eq. (3) gives the following relationship for non-isothermal degradation corresponding to the given conversion:

$$g(\alpha) = \int_0^{T_\alpha} \frac{d\alpha}{f(\alpha)} = \frac{A_\alpha}{\beta}\int_0^{T_\alpha} \exp\left(-\frac{E_\alpha}{RT}\right)\, dt \quad (4)$$

At non-isothermal condition:

$$\frac{1}{\beta}\int_0^{T_\alpha} \exp\left(-\frac{E_\alpha}{RT}\right)\, dT - \frac{1}{\beta_0}\int_0^{T_{\alpha,0}} \exp\left(-\frac{E_\alpha}{RT}\right)\, dT = 0 \quad (5)$$

where T_α and E_α are experimental values of the temperature and activation energy, respectively corresponding to a given conversion at heating rate of β. $T_{\alpha 0}$ found as a solution of Eq. (5) is a temperature at which a given conversion will be reached at an arbitrary heating rate, β_0. Solving Eq. (5) for different conversion, dependency of α on T at an arbitrary heating rate can be predicted and the experimental data are simulated in this way [7,20].

2.1. Flynn-Wall-Ozawa method

This integral method is an iso-conversional method in which the activation energy is estimated without the knowledge of reaction model. This method is useful for the kinetics interpretation of the TG data obtained from complex reactions. From Eq. (3) and Doyle approximation [21], the result of the integration is:

$$\ln\ \beta = \ln\left(\frac{AE}{R}\right) - \ln g(\alpha) - 5.3305 - 1.052\left(\frac{E}{RT}\right) \quad (6)$$

This equation generates a straight line when $\ln\beta$ is plotted against $1/T$ for iso-conversional fractions. The slope of the line will be equal to $-1.052(E/R)$ during a series of measurements with different heating rates at a fixed degree of conversion. If the determined activation energy changes with increasing of conversion, the existence of a complex reaction mechanism can be concluded. Otherwise a simple-step reaction may be occurred during pyrolysis.

2.2. Analytical model fitting method

To study the degradation mechanisms of the samples, in Eq. (4) various expression of differential, $f(\alpha)$, and integral, $g(\alpha)$, forms of the different solid state mechanisms have been proposed [7,15,16] (Table 1) and several analytical models have been used to estimate the Arrhenius parameters. One of such models is Coats–Redfern equation [22]:

$$\ln\frac{g(\alpha)}{T^2} = \ln\left[\frac{AR}{\beta E}\left(1 - \frac{2RT}{E}\right)\right] - \frac{E}{RT} \quad (7)$$

Considering that $\ln(1 - 2RT/E) \to 0$ for Doyle approximation [21], Eq. (7) is written as:

$$\ln\frac{g(\alpha)}{T^2} = \ln\left(\frac{AR}{\beta E}\right) - \frac{E}{RT} \quad (8)$$

Inserting different forms of $g(\alpha)$ into Eq. (8), results in a set of Arrhenius parameters. The linear plot of $\ln[g(\alpha)/T^2]$ versus $1/T$ makes it possible to determine E and $\ln(A)$ from the slope and intercept of the graph, respectively. It has been shown in some articles that the analytical model fitting method is unreliable and tends to yield meaningless kinetic parameters [7,23,24]. Furthermore, the solid state reactions are sensitive to many factors which are likely to change during process. Model-fitting methods (like Coats–Redfern method) are designed to extract a single set of Arrhenius parameters for the whole conversion ranges. These methods unable to reveal the complexity of the process in which the obtained average value of parameters do not reflect changes in the mechanism and kinetics with the temperature and conversion [23], while the Flynn-Wall-Ozawa (FWO) iso-conversional method is a free model technique which evaluate the dependence of the effective activation energy on conversion.

In this work the triplet kinetic parameters were obtained from the Coats–Redfern model fitting method, but the results were unre-

Table 1
Reaction mechanisms to represent the solid-state process [7,15,16]

Model	Symbol	$f(\alpha)$	$g(\alpha)$
Nucleation and nuclear growth			
Mapel unimolecular law	A1	$1-\alpha$	$-\ln(1-\alpha)$
Avrami–Erofe'ev equation	A2	$2(1-\alpha)[-\ln(1-\alpha)]^{1/2}$	$[-\ln(1-\alpha)]^{1/2}$
Avrami–Erofe'ev equation	A3	$3(1-\alpha)[-\ln(1-\alpha)]^{2/3}$	$[-\ln(1-\alpha)]^{1/3}$
Avrami–Erofe'ev equation	A4	$4(1-\alpha)[-\ln(1-\alpha)]^{3/4}$	$[-\ln(1-\alpha)]^{1/4}$
Diffusion			
Parabolic law	D1	$1/(2\alpha)$	α^2
Valenci equation	D2	$[-\ln(1-\alpha)]^{-1}$	$\alpha+(1-\alpha)\ln(1-\alpha)$
Jander equation	D3	$3(1-\alpha)^{1/3}/2[(1-\alpha)^{-1/3}-1]$	$[1-(1-\alpha)^{1/3}]^2$
Brounshtein–Ginstling equation	D4	$3/2[(1-\alpha)^{-1/3}-1]$	$1-(2\alpha/3)-(1-\alpha)^{2/3}$
Phase boundary controlled equation			
One-dimensional movement	R1	Constant	α
Contracting area	R2	$2(1-\alpha)^{1/2}$	$1-(1-\alpha)^{1/2}$
Contraction volume	R3	$3(1-\alpha)^{2/3}$	$1-(1-\alpha)^{1/3}$

liable, so the results of FWO iso-conversional method are reported in this article. Furthermore the isokinetic relationships method was used to evaluate the Arrhenius pre-exponential factor [20] and the results were compared with correlation method.

2.3. Isokinetic relationships (IKR) method

As it was mentioned before, the pre-exponential factor can be determined by assuming different reaction models (Table 1). In iso-conversional methods knowing of pre-exponential factor and reaction model is not required to identify the kinetic scheme of the process. A model-independent estimate of the pre-exponential factor can be obtained through the use of an artificial isokinetic relationship (IKR), in which in this method a common point of intersection of Arrhenius lines is defined as T_{iso} and k_{iso}. These values are isokinetic temperature and rate constant, respectively in which the relationship between these parameters is written below:

$$\ln(k_\varepsilon) = \frac{\ln(k_{iso}) - E_\varepsilon}{R(T_{iso}^{-1} - T^{-1})} \quad (9)$$

where the subscript ε refers to a factor that produces a change in Arrhenius parameters. In a general case the actual value of $\ln A_\alpha$ can be determined by this method:

$$\ln A_\varepsilon = a + bE_\varepsilon \quad (10)$$

where $a = \ln(k_{iso})$ and $b = (RT_{iso})^{-1}$ are coordinates of the intersection point of Arrhenius lines. It is important that this approach is based on a completely artificial IKR derived from results of the model-fitting method [7]. Intersection of the Arrhenius lines at nearly one point means that Arrhenius parameters will show a linear correlation:

$$\ln A_n = c + dE_n \quad (11)$$

where n refers to a particular reaction model (Table 1). When parameters c and d are determined, the E_α values are substituted to E_n in Eq. (11) to estimate the corresponding $\ln A_\alpha$ values [7,20].

3. Experimental

3.1. Materials

MMA and styrene (St) (Merck, Germany) were washed twice with 5 wt% aqueous solution of sodium hydroxide followed by washing twice with distilled water to eliminate the inhibitors. The monomers then were dried over anhydrous calcium sulfate. The drop stabilizer poly(vinyl alcohol) (PVA) with a degree of hydrolysis of 72.5% and a molecular weight of 75,000, tricalcium phosphate (TCP), benzoyl peroxide (BPO), potassium persulfate ($K_2S_2O_8$) and *tert*-butyl perbenzoate (TBPB) were provided by Merck (Germany) and used without purification. Sodium dodecylbenzene sulfonate $C_{18}H_{29}NaSO_3$ (DBSNa) (Fluka, Germany), were used as received. *n*-Pentane (Merck, Germany) was used as blowing agent.

Commercially available EPS with a density of 18–21 g/l was supplied by Tabriz petrochemical company (Tabriz, Iran).

3.2. Suspension copolymerization

The random copolymer of MMA with styrene (St) was synthesized by suspension copolymerization. For this copolymerization experiment, the vessel containing the monomers was purged by nitrogen. The required amount of PVA granules, TCP and DBSNa was added to the reactor containing pre-weighed amount of distilled deionized water and the mixture was kept stirred at ambient temperature for 2 h. The temperature of the mixture was raised to the reaction temperature. The dispersed phase was weighed and added to the reactor. The reaction was started with the aid of pre-dissolved initiator in the monomer phase and addition to the dispersion media. The MMA-St molar ratio in all runs was kept constant at 70/30. The impregnation stage was implemented by loading *n*-pentane in the reactor and diffusion into the softened beads at about 70% conversion of the monomers. This was followed by a high temperature–high pressure cycle and depending on the impregnation temperature (T_i) and pressure (P_i), a minimum time allowed for diffusion of the blowing agent to reach the core of the beads. The first stage polymerization was carried out at about 80 °C and ambient pressure, while the second stage was carried out at about 120 °C and 10 bars.

3.3. Copolymer analysis

The composition of the copolymer was calculated using the ^{1}H NMR spectra of the samples, which were obtained with a 500 MHz, BRÜKER (Advance DPX) NMR spectrometer.

Copolymer molecular weight was measured using Waters, Maxima 820 gel permeation chromatography (GPC) instrument.

3.4. Thermogravimetric analysis

TG analyses were carried out for MMA-St and EPS foams by a thermogravimetric analyzer (TGA). The experiments were carried out on a Perkin–Elmer Pyris Diamond TG/DTA analyzer to study the non-isothermal degradation kinetics. 5 mg of fully expanded lost foam (MMA-St copolymer or EPS) was placed in an aluminum crucible and heated from room temperature to about 600 °C under nitrogen purge with a flow rate of 100 ml/min at different heating rates of 10, 15, 20 and 25 °C/min and weight loss versus temperature was recorded.

4. Results and discussion

4.1. Copolymer composition and structure

The ^{1}H NMR spectrum of the MMA-St copolymer showed that the peaks at 7.1 and 3.6 ppm correspond to $-C_6H_5$ and $-OCH_3$ groups, respectively. The peak at 2.8 ppm, absent in the ^{1}H NMR spectra of both relevant homopolymers, [25] is observed in the copolymer spectrum. This has been assigned to the $-OCH_3$ group of MMA bonded to the St sequence [26]. Opresnik et al. [27] also showed that this peak could be much more clearly seen in the ^{1}H NMR spectra of a MMA-St random copolymer rather than in that of a MMA-St block copolymer. The molar ratio of MMA/St was kept 70/30 in the random copolymer.

Average molecular weights (M_n, M_w) and polydispersity index (PDI) for copolymer were, 4.9×10^4, 1.18×10^5 and 2.38, respectively.

4.2. Thermal degradation behavior

The weight loss versus temperature curves of dynamic thermal degradation of MMA-St copolymer and EPS foams obtained at different heating rates. The results showed that after 500 °C there is no residue in both foams and the conversion values practically reach to 1. In both foam, delay in degradation and shift of the curves to the higher temperatures with increasing of the heating rate is observed. It was evident that the thermal decomposition of MMA-St copolymer lost foam, proceeds uniformly in the temperature range of 150–500 °C. Due to release of the remained pentane or water from the copolymer, a small amount of weight loss is observed in the temperature range of 135–140 °C. In EPS foam, the weight loss

Table 2
Dynamic thermogravimetric data of MMA-St copolymer and EPS foams

Samples	β (°C/min)	T_{rel} (°C)	$T_{20\,wt\%}$ (°C)	T_{max} (°C)	$T_{95\,wt\%}$ (°C)
MMA-StMMA-St copolymer	10	135.55	277.54	308.77	385.91
	15	136.33	285.256	318.78	388.67
	20	137.17	285.798	324.08	392.70
	25	138.75	292.44	327	394.64
EPS	10	125.1	320.04	349.76	390.27
	15	125.2	337.18	365.58	403.63
	20	126.1	342.94	370.1	406.11
	25	127.5	364.05	392	423.46

in this temperature range is very small and cannot be observed in TG curves.

The results of 20% and 95% weight loss temperatures, maximum reaction rate temperature T_{max} as well as pentane gas releasing temperatures (T_{rel}), for both lost foams at different heating rates, are listed in Table 2.

For instance, 20% weight loss temperature ($T_{20\,wt\%}$) for MMA-StMMA-St copolymer and EPS at $\beta = 10$ °C/min, are 277.54 and 320.04 °C, respectively. With increasing of heating rate, $T_{20\,wt\%}$ values increase in both foams. $T_{20\,wt\%}$, T_{max} and $T_{95\,wt\%}$ for MMA-St lost foam are lower than the corresponding temperatures for EPS foam in all heating rates. The presence of ($-COOCH_3$) functional group in the structure of MMA-St copolymer, indicates that this foam starts to degrade earlier, compared to EPS foam. The rate of degradation depends on the heating rate. Comparative degree of conversion, α, versus temperature curves of both foams, at $\beta = 10$ and 25 °C/min, are shown in Fig. 1.

These figures precisely show that the decomposition initiation temperature and rate of weight loss for copolymer foam is lower than EPS in both heating rates. Clearly, EPS foam is thermally more stable than copolymer foam, because the thermal decomposition of EPS foam initiates at higher temperatures compared to copolymer foam. On the other hand, its thermal degradation goes on in a narrower temperature interval than copolymer. It means that the degradation of EPS foam may occur faster than copolymer foam and due to special unknown mechanism in this random copolymer foam degradation process, the rate of weight loss for copolymer is always lower than EPS. This may be ascribed to the incorporation of MMA into St in copolymer that interfere with the degradation mechanisms of MMA and St and affect the degradation pathway of copolymer lost foam [1,28].

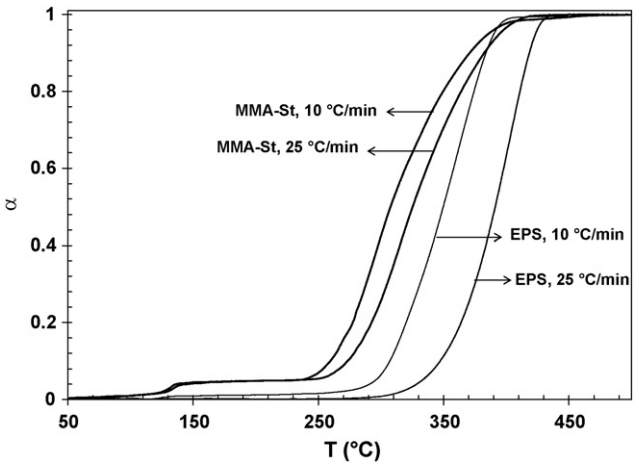

Fig. 1. Conversion versus temperature curves of MMA-St copolymer and EPS foams at $\beta = 10$ and $\beta = 25$ °C/min.

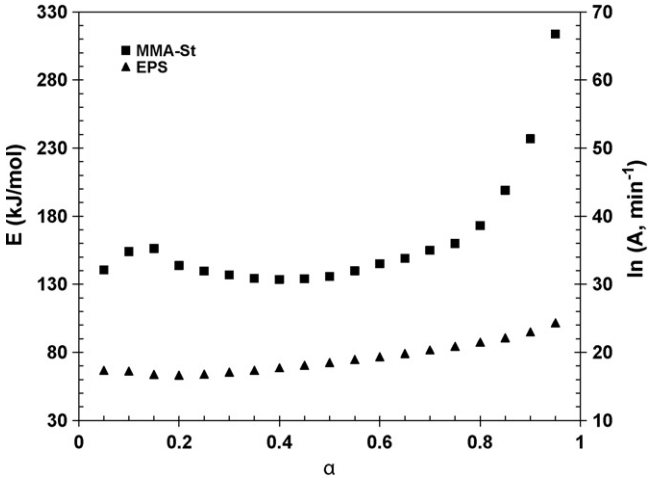

Fig. 2. Variation of activation energy (E) and pre-exponential factor ($\ln A$) versus conversion for both lost foams.

4.3. Degradation kinetics

TG curves (Fig. 1) show that after $T = 160$ °C, the weight loss becomes stable for copolymer and EPS lost foams. To eliminate the effect of pentane and water release on the degradation kinetics, the weight loss before $T = 160$ °C was ignored and the degree of conversion was modified for kinetics calculations in all heating rates.

The Flynn-Wall-Ozawa analysis ($\ln\beta$ versus $1/T$ curves) for the conversion values in the range of 5–95% were conducted on both MMA-St and EPS lost foams. These results showed that the best fitting straight lines are nearly parallel for various heating rates. Activation energies, E, corresponding to the different conversions, determined from the slope of these lines, are shown in Fig. 2 for MMA-St as well as EPS lost foams.

In the case of MMA-St foam, the values of E increase in the range of $0.05 \leq \alpha \leq 0.15$ then decrease in the range of $0.15 \leq \alpha \leq 0.70$ and finally increase to 313.74 kJ/mol in $\alpha = 0.95$. The variation of activation energy versus conversion is an evidence of the complex degradation mechanism (probably parallel or consecutive reactions [7,20,29]) of MMA-StMMA-St copolymer foam. This behavior was observed in the range of $0.05 \leq \alpha \leq 0.15$, $0.40 \leq \alpha \leq 0.70$ and so distinctly in the range of $0.70 \leq \alpha \leq 0.95$.

For EPS lost foam, the values of E decrease to 63.24 kJ/mol at $\alpha = 0.20$ and then increase regularly in the conversion range of 20–95% to 105 kJ/mol. This behavior is an evidence of multi-steps degradation reactions and consequently changing of the reaction mechanisms at the selected conversion range.

Vyazovkin and Lesnikovich [30] showed that revealing the dependence of activation energy on conversion helps not only to disclose the complexity of a pyrolysis process, but also to identify its kinetic scheme. An increasing dependence of E on α is found for competing reactions, some independent and consecutive reactions or the decreasing dependence of E on α corresponds to the kinetic scheme of an endothermic reversible reaction followed by an irreversible one [20]. The concave shape of decreasing of E on α can correspond to changing the mechanism from kinetic to a diffusion regime [7,20]. In this work according to Fig. 2, nearly increasing shape of E versus α is observed in thermal degradation of both foams, so that the diffusion degradation mechanisms (Table 1) were ignored in the following calculations. Furthermore the values of E for MMA-St copolymer foam in whole conversion ranges are higher than EPS foam.

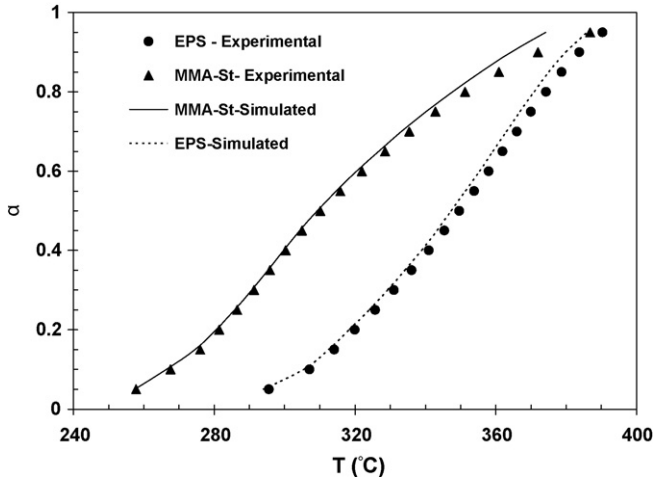

Fig. 3. Simulated and experimental conversion versus temperature plots for thermal degradation of MMA-St and EPS foams in conversion range of 0.05–0.95.

The simulated curves of α–T by Eq. (5) are plotted in Fig. 3 for both lost foams compared with the corresponding experimental data. The absence of both the kinetic model and the pre-exponential factor in Eq. (5) means that these parameters do not introduce errors of their evaluation into the solution of applied kinetic problems [20].

Based on the various reaction mechanisms given in Table 1, the kinetics parameters obtained from the non-isothermal TG data for MMA-St copolymer and EPS foams, using Coats–Redfern equation (model-fitting method), are given in Table 3. These data are used in isokinetic calculations.

The results of Table 3 obviously indicate the strong dependence of the kinetics parameters on the selected reaction mechanism. These data reveal that the correlation factor of A4 and R1 are lower compared to the other models, which have correlation factor between 0.89 and 0.95. It means that when the correlation factors are as standard measure, A1 and A2 mechanisms are probable for degradation of MMA-St copolymer foam due to their high correlation factors. Therefore it is difficult to make a decision about exact thermal degradation mechanism. In the case of EPS foam, almost the correlation factors for A_n type models are in acceptable ranges. On the other hand, the correlation factors for R_n type models are lower than those for other mechanisms in degradation of both foams. As it is clear from Table 3, the values of Arrhenius parameters corresponding to those models that have high correlation factors vary significantly. Such an uncertainty in the kinetic parameters cannot lead to suitable kinetic predictions and reasonable mechanism. Also as mentioned in theoretical section, the model-fitting method results in only one single pair of Arrhenius parameters in which the most solid state reactions are not simple one-step processes and consist of multiple steps during pyrolysis process.

Table 3
Arrhenius parameters for non-isothermal pyrolysis of MMA-St copolymer and EPS foams at 10 °C/min

Foam samples	Mechanism	E (kJ/mol)	$\ln A$ ($\min^{-1}$)	Correlation factor
MMA-St copolymer	A1	73.35	13.1340	0.9498
	A2	31.75	4.0384	0.9322
	A3	17.89	0.7119	0.9050
	A4	10.96	−1.1543	0.8605
	R1	48.00	7.1021	0.8317
	R2	59.19	9.1020	0.8983
	R3	63.56	9.7342	0.9176
EPS	A1	116.37	21.05887	0.9920
	A2	53.08	8.2476	0.9901
	A3	31.98	3.7322	0.9876
	A4	21.43	1.3275	0.9840
	R1	83.49	13.9655	0.9444
	R2	98.25	16.4607	0.9747
	R3	103.9	17.2771	0.9821

To determine $\ln A$ versus alpha for E versus alpha shown in Fig. 2, all $\ln A$ and E data for MMA-St and EPS foams from Table 3 were taken and find respective correlations $\ln A = aE + b$. Then E values were taken from Fig. 2 and substitute in respective correlation for MMA-St and EPS foams. In this study as well as IKR method [20] was used to determine $\ln A$ versus alpha, but the results were the same as the correlation method.

For reconstruction the reaction model numerically, knowing both values of $\ln A_\alpha$ and E_α is necessary in which these kinetic parameters were determined for any degree of conversion. Substituting these kinetic parameters into Eq. (4), the form of reaction model ($g(\alpha)$), can be reconstructed. The important problem is that this interpretation of reaction model is meaningful for a single-step process in which the E values are independent of α. In this work, as it was demonstrated before, the activation energy values change with degree of conversion significantly indicating the presence of multiple-step reactions in thermal degradation of both foams. Therefore it seems that such reconstruction of reaction model (numerically and from Table 1), is not reliable.

5. Conclusion

The thermal decomposition of MMA-St copolymer and EPS foams under nitrogen purge and at different heating rates has been studied by thermogravimetry in non-isothermal condition. The presence of functional group of ($-COOCH_3$) in MMA-St copolymer, is an indication that this foam starts to degrade earlier, compared to EPS foam. The initiation decomposition temperature and rate of weight loss for copolymer foam is lower than EPS at all heating rates. The main reason for this behavior was the interference of degradation mechanisms of MMA and St in copolymer which affects the pathway of degradation process for copolymer foam. The complexity of the pyrolysis reaction was shown by the iso-conversional method in which the apparent activation energy was changed with degree of conversion for both foams. It was concluded that the activation energy calculated by FWO method in any degree of conversion, for MMA-StMMA-St copolymer foam was higher than EPS foam. In this work the kinetic triplets obtained from the proposed reaction-order model have been determined. The results show that the iso-conversional method allows reliable prediction of kinetic scheme for all conversion ranges. Furthermore the values of $\ln A_\alpha$ were determined using correlation method. As a conclusion, the model-free methods can be suggested as a suitable way of determining consistent kinetic parameters.

Acknowledgments

The authors gratefully acknowledge from Sahand University of Technology and Iran Tractor Foundry Company for financial support. The authors would also like to gratefully acknowledge from the research project team members of Institute of Polymeric Materials: Mr. Kyumars Jalili and Mr. Mortaza Nasiri for their involvement and encouragement.

References

[1] P. Kannan, J.J. Birnacki, D.P. Visco, J. Anal. Appl. Pyrol. 78 (2007) 162–171.
[2] M. Ghasemi, Characterizing the lost foam copolymer properties and comparing with expandable polystyrene. MSc. Thesis. Sahand University of Technology, Tabriz, Iran (2006).
[3] B.N. Jang, C.A. Wilkie, Polymer 46 (2005) 2933–2942.

[4] B.S. Kang, S.G. Kim, J.S. Kim, J. Anal. Appl. Pyrol. 81 (2008) 7–13.
[5] R.S. Lehrle, D.J. Atkinson, D.M. Bate, P.A. Gardner, M.R. Grimbley, S.A. Groves, E.J. Place, R.J. Williams, Polym. Degrad. Stab. 52 (1996) 183–196.
[6] J.D. Peterson, S. Vyazovkin, C.A. Wight, J. Phys. Chem. B 103 (1999) 8087–8092.
[7] S. Vyazovkin, C.A. Wight, Annu. Rev. Phys. Chem. 48 (1997) 125–149.
[8] B.J. Holland, J.N. Hay, Thermochim. Acta 388 (2002) 253–273.
[9] J. Ceamanos, J.F. Mastral, A. Millera, M.E. Aldea, J. Anal. Appl. Pyrol. 65 (2002) 93–110.
[10] W. Kaminsky, C. Eger, J. Anal. Appl. Pyrol. 58 (2001) 781–787.
[11] Z. Gao, T. Kaneko, I. Amasaki, M. Nakada, Polym. Degrad. Stab. 80 (2003) 269–274.
[12] M.N. Radhakrishnan Nair, G.V. Thomas, M.R. Gopinathan Nair, Polym. Degrad. Stab. 92 (2007) 189–196.
[13] A.C. Lua, J. Su, Polym. Degrad. Stab. 91 (2006) 144–153.
[14] J.T. Sun, Y.D. Huang, G.F. Gong, Polym. Degrad. Stab. 91 (2006) 339–346.
[15] S. Ma, J.O. Hill, S. Heng, J. Therm. Anal. Calorim. 37 (1991) 1161–1171.
[16] F. Fraga, E.R. Nunez, J. Appl. Polym. Sci. 80 (2001) 776–782.
[17] J.H. Flynn, L.A. Wall, J. Res. Natl. Bur. Stand. 70A (1996) 487–523.
[18] T. Ozawa, J. Bull, Chem. Soc. Jpn. 38 (1965) 1881–1889.
[19] J.E. House, Principles of Chemical Kinetics, WMC., Brown Publishers, Dubuque, 1997, p. 37.
[20] S. Vyazovkin, Int. J. Chem. Kinet. 28 (1996) 95–101.
[21] H. Wang, J. Yang, S. Long, X. Wang, Z. Yang, G. Li, Polym. Degrad. Stab. 83 (2004) 229–235.
[22] A.W. Coats, J.P. Redfern, Nature 201 (1964) 68–69.
[23] S. Vyazovkin, C.A. Wight, Thermochim. Acta. 340–341 (1999) 53–68.
[24] S. Vyazovkin, N. Sbirrazzuoli, Macromol. Rapid Commun. 27 (2006) 1515–1532.
[25] A. Kongkaew, J. Wootthikanokkhan, J. Appl. Polym. Sci. 75 (2000) 938–944.
[26] P.N.A. Songkhla, J. Wootthikanokkhan, J. Polym. Sci., Polym. Phys. 40 (2002) 562–571.
[27] M. Opresnik, A. Sebenik, Polym. Int. 36 (1995) 13–22.
[28] L. Zhang, G. Liu, R. Ji, Y. Yao, X. Qu, L. Yang, Gao, Polym. Int. 52 (2003) 74–80.
[29] P. Budrugeac, Polym. Degrad. Stab. 89 (2005) 265–273.
[30] S.V. Vyazovkin, A.I. Lesnikovich, Thermochim. Acta. 165 (1990) 273–280.